Clim. Past Discuss., 8, 2607–2644, 2012
www.clim-past-discuss.net/8/2607/2012/
doi:10.5194/cpd-8-2607-2012

Climate of the Past Discussions

Past climate changes and permafrost depth at the Lake El'gygytgyn site: implications from data and thermal modelling

D. Mottaghy[1], G. Schwamborn[2], and V. Rath[3]

[1]Geophysica Beratungsgesellschaft mbH, Aachen, Germany
[2]Alfred Wegener Institute for Polar and Marine Research, Potsdam, Germany
[3]Department of Earth Sciences, Astronomy and Astrophysics, Faculty of Physical Sciences, Universidad Complutense de Madrid, Madrid, Spain

Received: 6 July 2012 – Accepted: 9 July 2012 – Published: 16 July 2012

Correspondence to: D. Mottaghy (d.mottaghy@geophysica.de)

Published by Copernicus Publications on behalf of the European Geosciences Union.

Abstract

We present results of numerical simulations of the temperature field of the subsurface around and beneath the crater Lake El'gygytgyn in NE Russia, which is subject of an interdisciplinary drilling campaign within the International Continental Drilling Program (ICDP). This study focuses on determining the permafrost depth and the transition between talik and permafrost regimes, both, under steady-state and transient conditions of past climate changes. Thermal properties of the subsurface are deduced from measurements on three representative core samples taken from the quaternary sediments and the underlying impact rock. Further information is derived from the available geophysical logs and literature data. The temperature data from the lake borehole ICDP site 5011-1 down to 400 m depth below lake bottom are dominated by thermal perturbations related to the drilling process, and thus only give reliable values for the lowermost value in the borehole. Undisturbed temperature data recorded over more than two years in the 140 m deep land-based borehole ICDP site 5011-3 allow to determine the mean annual ground surface temperature (GST), as well as its history (GSTH) to a certain extent. Although the borehole's depth is by far not sufficient for a complete reconstruction of past temperatures back to the last glacial maximum (LGM), the temperature data and our modelling results show that there is still an influence of the LGM on the thermal regime, and thus on the permafrost depth. Whereas the latter result is obtained from the deeper part of the temperature profile, the rather strong curvature of the temperature data in shallower depths around 30 m can be explained by a comparatively large amplitude of the Little Ice Age (LIA), with a subsequently persistent cool period. Other mechanisms like varying porosity may also have an influence on the temperature profile, however, our modelling studies imply a major contribution from recent climate changes.

1 Introduction

The crater Lake El'gygytgyn in NE Russia (67° 30′ N, 172° 5′ E, 492 m a.s.l.) was formed by an Asteroid impact 3.6 Myr ago (Fig. 2). In 2008, an interdisciplinary drilling campaign was carried out that is part of the International Continental Drilling Program (ICDP). Detailed information on this project re described by, while the most important paleoclimatological were published by Melles et al. (2012). The primary aim is to obtain the currently longest time-continuous sedimentary record of climate change in the terrestrial Arctic, which will improve the understanding of the Arctic climate evolution in the late Cenozoic, when related to data from other marine and terrestrial sites. Additionally, the collection of meteorite impact rocks from a metavolcanic bedrock terrain are expected to produce unique insights on the impact processes that might be found on other planets. In accordance with these goals, boreholes were drilled at two sites, one near the deepest part of the lake (ICDP site 5011-1), and the other on land close to its shoreline (ICDP site 5011-3). From borehole 5011-1 315 m of sediment cores were retrieved, complemented by 200 m from the underlying volcanic bedrock, while from 5011-3 a 141.5 m long permafrost core composed of frozen deposits was recovered (Fig. 2).

In this paper, we focus on the characterization of the thermal field beneath and around the lake, studying the influence of variations of thermal properties and past ground surface temperature changes by numerical modelling (e.g. Osterkamp and Gosink, 1991; Galushkin, 1997; Mottaghy and Rath, 2006; Holmén et al., 2011). In the recent years, the impact of climate change on permafrost formation and evolution has become a particular subject of interest. The understanding of the response of permafrost regimes to transient changes in surface temperatures is a key issue regarding the prediction of the influence of global warming on permafrost areas (Saito et al., 2007; Lemke et al., 2007; Serreze et al., 2007; Miller et al., 2009, 2010b; Serreze and Barry, 2011, amongst many others).

When studying heat transfer in the Earth's upper crust, the upper boundary condition of heat transport is determined by the local climatic conditions. The variations of this condition induces a transient signal which diffuses into the subsurface. Thus, ground temperatures may be seen as an archive of past climate signals. Reconstructing the past changes is of major interest since one of the most important components of climatic change is the variation of temperature at the Earth's surface. However, the diffusive character implies that the older the signal is, the more it is attenuated, with a corresponding larger uncertainty in magnitude and timing. Analysing the variation of temperature with depth, past fluctuations at the Earth's surface can be reconstructed to a certain extent (see, e.g. the recent review by González-Rouco et al., 2009, and the references therein). This reconstruction can be performed by numerical forward modelling with models of varying complexity, or inverse methods in the narrow sense (Shen and Beck, 1991; Beltrami and Mareschal, 1991; Beck et al., 1992; Rath and Mottaghy, 2007, amongst others). A prerequisite for such a reconstruction is sufficient available data, most relevant temperature data. Here, we limit ourselves to forward modelling for determining the present day temperature profile, because the available temperature data is not sufficient for a reliable reconstruction of the ground surface temperature history (GSTH) at the study area. Nevertheless, we propose that the combination of forward modelling and sensitivity studies allow some meaningful conclusions concerning the local GSTH.

As our approach relies on forward modelling, we must assume a certain GSTH driving the simulations. In particular, it has been shown (Rath et al., 2012) that the amplitude of the last glacial maximum and the following warming from Pleistocene to Holocene influence the temperature distribution even in the upper surface. However, in the arctic region the values of this amplitude are not well known, but the available data suggest a 18 ± 7 K cooler mean temperature than today (Miller et al., 2010a,b). There have been some efforts to determine the spatial distribution of this parameter (Demezhko et al., 2007) whose results also enter our models, but the available data in the area is sparse. In order to do justice to these uncertainties, we perform Monte

Carlo simulations with an ensemble of GSTHs as boundary conditions for the transient forward modelling.

At middle and high latitude sites like the Lake El'gygytgyn, freezing and thawing processes may create a considerable effect on subsurface temperature-depth profiles when climatic changes take place in time-scales of glaciations. Therefore, latent heat effects must be included in modelling studies in such areas. Depending on the amount of pores and fractures in rocks, and the fluids filling them, freezing and thawing will play an important role in controlling the subsurface thermal conditions when climatic changes take place in the ground surface temperature (Mottaghy and Rath, 2006; Rath and Mottaghy, 2007). This implies that the reconstruction of past temperatures by forward or inverse methods must include the freezing and thawing processes.

2 Available data

The data used for this study originate from the aforementioned boreholes, one in the deepest part of the lake (ICDP site 5011-1, depth 517 m below lake bottom), and one close to its shoreline (ICDP site 5011-3, depth 140 m below surface). Figure 1 shows the location of the Lake El'gygytgyn as well as a panorama view. Figure 2 gives an schematic sketch of the basin, and of the site and the boreholes' locations. Our investigations rely on (a) temperature measurements in both boreholes; (b) determination of thermal properties from laboratory measurements on cores and γ-ray logging in borehole 5011-1.

The temperature data from the lake borehole ICDP site 5011-1 are considered disturbed, and only the value from the lowermost part is supposed to approximate the undisturbed temperature of the surrounding bedrock (see Sect. 4). Temperature measurements in the permafrost hole 5011-3 started shortly after its drilling in November–December 2008. The earliest recordings were expected to reflect conditions undisturbed by the physical effects of the drilling process. However, temperatures around $-6\,^{\circ}$C were determined at depths which are not affected by daily or seasonal variations.

Subsequently, during the years from 2008 to 2010, temperatures were continuously recorded by an automatic data logger in this borehole, in order to monitor the approach of the subsurface temperatures to conditions in equilibrium with the ambient rock. These measurements confirm the first measurements, showing that the value obtained earlier was already rather near to the equilibrium value. In Fig. 3, a selection of the recorded temperatures in the year 2010 is plotted. It can be seen that in depth ranges between 15 and 20 m annual variations disappear. Our modelling studies target at the impact of long term climate changes on the temperature field, and in consequence annual variations in the uppermost layers are not taken into account. At a depth 20 m the average temperature for this year was estimated to −5.9 ± 0.1 °C. This estimate was on turn used to extrapolate a value for the upper boundary condition of the modelling studies of −6.7 °C at the surface.

Regarding the thermal properties of the prevailing sediments and rocks in frozen condition, we performed thermal conductivity measurements on one core sample retrieved from borehole 5011-3: No. 28(2) at 28.15–28.35 m depth. This sample consists of sandy gravel, and is representative for much of the material from the permafrost core (Schwamborn et al., 2012) associated with the model's unit 2 in Fig. 2. We used the full space and half space line source measuring device (TK-04, TeKa, Berlin), the measurement procedures is described by Erbas (2001). Other studies (e.g. Putkonen, 2003) show that the determination of frozen soil thermal properties by a needle probe yields reasonable results. The work flow, elaborated together with the manufacturer, was as follows: first, a part of the frozen core, which consists of loose sand and gravel as well as the ice fraction, was cut off and put in a jar where it was left to thaw. Then, thermal conductivity was determined with the needle probe in the common procedure. To ensure reliable results, several heating cycles were applied. This allowed to pick only stable solutions, and also made it possible to determine a mean value along with a standard deviation.

After finishing the measurements on the thawed material the mixture was frozen with the needle probe remaining in it. Then, thermal conductivity was determined for

CPD
8, 2607–2644, 2012

Lake El'gygytgyn site: thermal modelling

D. Mottaghy et al.

the frozen mixture. Finally, the mixture was unfrozen once more and put in the half space line source. In contrast to the full-space line source there is less triggering of possible convection since the heating source lies on top of the sample mixture. The results shown in Table 1 confirm this assumed bias: whereas the “unfrozen” values of the full-space line source feature quite some variation as seen by the standard variation, the values of the frozen mixture is more stable. Furthermore, thermal conductivity measured by the half-space probe is slightly lower. Porosity was determined by using a defined volume and weighing the saturated and dry sample. This allows to determine the matrix thermal conductivity, using the geometric mixing law, which proved to be a good theoretical description of the effective thermal conductivity of rocks with different components (e.g. Hartmann et al., 2008).

Further measurements were performed in order to determine thermal conductivity of the impact rocks of unit 4 (polymictic and suevitic breccia) and unit 5 (monomictic breccia and fractured bedrock). Two samples were chosen, originating from 334 m (No. C104) and 491 m (No. C170) below lake bottom, respectively. We used the optical scanning method (TCS). A detailed description and comparison with other methods can be found in Popov et al. (1999). Thermal conductivity was determined in the original dry state of the sample, after being completely dried, and after being saturated again. The latter two measurement procedures allowed to estimate the porosity of the sample. Table 2 lists the result.

3 Numerical model

The finite difference (FD) code SHEMAT_SUITE (Rath et al., 2006) was used for the 2-D numerical simulation of heat transport processes at the Lake El’gygytgyn site. As mentioned above, in addition to assuming all thermal properties to be functions of temperatures, latent heat effects due to freezing and thawing of subsurface fluids are accounted for in the code. Particularly, the freezing range can be adapted, taking into account that the phase change occurs over a temperature range in the subsurface, assuming a functional relationship between unfrozen water content an temperature given by Lunardini (1988). Water and ice properties in the freezing domain were calculated using the formulations of Fukusako (1990) and Ling and Zhang (2004). A detailed description of this approach is found in Mottaghy and Rath (2006).

3.1 Conceptual model

For building the numerical model, the basin scheme shown in Fig. 2 is used as a basis. This scheme is based on seismic basin profiling (Gebhardt et al., 2006).

The thermal properties of the different zones were derived from our own measurements (see Sect. 2), as well as literature data. Core sample 28(2) is assumed to be representative for the lacustrine sediments of unit 2 in Fig. 2. We deduced some information from the available studies such as Asikainen et al. (2007) on grain size, clay mineralogy, and crystallinity to assess the thermal properties of the lake sediments. Together with a γ-ray log from borehole ICDP site 5011-1 (Gebhardt et al., 2010), and using literature data we estimate thermal conductivity as summarized together with other properties in Table 1. The lacustrine sediments are likely to exhibit lower values of bulk thermal conductivity which is mainly due to high porosities around 35 % (Melles, 2006). The impact rocks in unit 3 and unit 4 show higher γ-ray values (around 150 gAPI) which implies some quartz content of the suevite bedrock. This is confirmed by the measurements of the two samples from the impact bedrock, and is consistent with results on comparable rocks (Popov et al., 2003; Mayr et al., 2008). Bulk thermal conductivity becomes higher along with lower porosity in the impact rocks. For the transient simulations, additionally volumetric heat capacity must be considered. Here, we use the general mean value of 2.3 $\mathrm{MJ\,m^{-3}\,K^{-1}}$ as given in Beck (1988). With respect to internal heat generation of the rocks, we assume a general value of 0.5 $\mathrm{\mu W\,m^{-3}}$ for the lake sediments and 1 $\mathrm{\mu W\,m^{-3}}$ for the impact rock. However, this parameter plays only a secondary role since our model only considers the upper few hundred metres of sediments and bedrock which is not enough for a significant influence of heat generation on the temperature field. Table 3 summarizes some properties of the numerical model.

All thermal properties, in particular thermal conductivity, represent initial values for the subsequent modelling studies, but had to be slightly adapted for the simulations presented in Sect. 5 in order to fit the observations.

3.2 Boundary conditions

The current mean annual air temperature (MAAT) in the area is −10.3 °C (Nolan and Brigham-Grette, 2007; Nolan, 2012), which is a lower boundary condition for the mean annual ground surface temperature (GST). The coupling between air and ground surface temperature is not trivial and has been studied for some decades now (e.g. Smerdon et al., 2004, 2006; Stieglitz and Smerdon, 2007). In particular in areas with varying snow cover, several parameters play a role (Kukkonen, 1987). Generally, the mean annual GST is some degrees above the mean annual air temperature. A recent study (Ge et al., 2011) presents numerical modelling of the different coupling mechanisms between air, soil, and groundwater flow in a permafrost area, the Northern Central Tibet Plateau. Although this site is not directly comparable to the Lake El'gygytgyn area, the available data confirms a 3–4 K higher mean annual GST compared to the MAAT: as explained in Sect. 2, the long term measurements in borehole 5011-3 allow to determine the mean annual GST at the study site, it is about −6 °C at 20 m depth.

For the transient simulations we use a ground surface temperature history (GSTH) as discussed in Sect. 5. At the lake floor, a mean temperature of 5.5 °C is set, which is supported by some temperature data (see Sect. 3). Whereas the bottom lake water approaches 4 °C, the value where water density is highest, the higher temperature value in the uppermost lake sediment layers may point to a seasonal signal that has been preserved from previous warmed up summer water masses. It is known from subglacial lakes in Antarctica without seasonal cycling that water temperatures at the bottom of this kind of lakes remain at 4 °C at maximum with only slight variation (Vincent and Laybourn-Parry, 2008). Water levels change on long-term scales. For instance, it is well documented that the level was some 10 m lower at the LGM (Juschus et al., 2011). However, when comparing this range of water level change with the total water depth of up to 175 m in Lake El'gygytgyn it is negligible to account for that in terms of changing water mass circulation during the last 125 kyr which are studied here. Instead, we accept the measured value of 5.5 °C as a reasonable value for the upper lake sediment environment (see Sect. 4).

The lower boundary condition is an estimated basal heat flow, there is no data in the vicinity of the study area. The compilation of global heat flow data of Pollack et al. (1993) lists a few data, which originate from boreholes some 500 km away. Yershov (1998), referring to Russian sources, presents a heat flow map with values between 40 mW m^{-2} and 80 mW m^{-2} for this area. Recently Goutorbe et al. (2011) published a new compilation of global heat flow, combining the data of Pollack et al. (1993) with geological proxies, applying different interpolation techniques. From their findings the surface heat flow in the area is 66 ± 8 mW m^{-2}. Therefore, we initially set the lower boundary condition to this value and compare the results to the available temperature data (see Sect. 4).

4 Steady-state simulations

In order to determine the temperature field near and beneath lake, we performed steady state simulations as a first step. All the parameters described in Sect. 3.2 enter the numerical modelling. In particular, both the temperature profile in the permafrost borehole as well as the lake borehole give valuable constraints to the upper and lower boundary conditions. However, the data from the lake do not represent undisturbed conditions. Thus, the data is restricted to some general temperature gradient, because the temperature measured in the lowermost part (400 m below lake surface) should be most reliable (Kueck, 2010, personal communication). The different logs and the assumed gradient are shown in Fig. 4. Therefore, we used this value (about 25 °C) to test the initially assumed basal heat flow (see Sect. 3.2). However, it only slightly varied, changing from initial value of 66 mW m^{-2} to 70 mW m^{-2}, which is still within the uncertainty range given in Goutorbe et al. (2011). Therefore we can conclude that the input

CPD
8, 2607–2644, 2012
Lake El'gygytgyn site: thermal modelling
D. Mottaghy et al.

parameters of our model represent a reasonable basis for the subsequent modelling studies.

In contrast to the lake hole temperature data, the long term record in borehole 5011-3 reflects undisturbed conditions, but the shallow depth (140 m) only allows a limited calibration with respect to the thermal properties of the layers beneath. Furthermore, transient effects such as paleoclimatic ground surface temperature changes are likely to have a significant influence on the temperature field, as described in Sect. 5. Thus, the measurements on thermal conductivity give valuable constraints for a reliable temperature modelling.

Figure 5 shows the modelled temperature profiles in comparison with the data plotted in Fig. 4 at borehole 5011-1 in the lake, as well as at the land location, borehole 5011-3. The dashed and dotted lines show the strong sensitivity to thermal conductivity. The values are varied within the ranges given in Table 4. The lower and higher thermal conductivity values yield a higher and lower temperature gradient, respectively. This variation in thermal conductivity is rather large: due to our measurements, the actual values are likely to be close the mean values, represented by the solid lines in Fig. 5.

It is important to notice that steady-state simulations can explain temperature distribution beneath the lake, applying thermal conductivity values determined in the lab and from the literature. As explained in Sect. 3.2, the lowermost temperature value is considered to be representative and can be well reproduced by the model. However, the steady-state simulations are not able to explain the temperature profile of the permafrost borehole 5011-3 (Fig. 5). Even with a variation within a rather large uncertainty range of ±20 % is insufficient to match the measured data. Therefore, transient surface temperature changes must be taken into account.

In Fig. 6 the units and the temperature field of the whole model are shown, again applying different thermal conductivity values in order to demonstrate the sensitivity of the temperature field to this parameter. The lower boundary of permafrost (0 °C isoline) is highlighted in order to visualise the sensitivity to thermal conductivity.

CPD
8, 2607–2644, 2012

5 Transient simulations

In order to study the influence of past climate variations, we performed transient simulations, applying a simple boxcar model for the climate changes in the past 125 000 yr (Fig. 7). For this, we used the available information on the past climate as described in Sect. 1. From pollen records only vegetation and thus information on summer climate conditions can be reconstructed, which is obviously only a partial contribution to the mean annual air temperature. Furthermore, the duration, thickness and kind of snow cover play a role in the coupling between air and ground surface temperatures (see Sect. 3.2). As the study site seemed to remain without glacier cover, very low temperatures during the LGM are likely to have prevailed (e.g. Miller et al., 2010a). Therefore, a rather large amplitude of the Pleistocene-Holocene temperature step is likely and confirmed by our modelling results: in order to explain the temperature variation with depth in the lower part of the measured profile, the amplitude of the LGM (denoted as PGW Fig. 7) is estimated to be around 14 K, which is in agreement with the results from other studies (see Sect. 1).

The results are shown in Fig. 8. This figure also shows the situation at the end of the LGM when permafrost depth was obviously much larger. Today, our modelling results suggest a permafrost base of approximately 340 m depth at the borehole 5011-3. Compared to the results from the steady-state simulations, it becomes evident that the past changes in GST have a significant influence on the temperature distribution today. Table 5 summarises the different results for this value at the permafrost borehole 5011-3.

The upper part of the measured profile in borehole 5011-3 shows some strong curvature (see blue lines Fig. 8), which was thoroughly investigated by sensitivity studies in terms of more recent surface temperature changes. Other possible influences are unknown heterogeneities in thermal parameters, porosity changes, or fluid flow. However, these can be largely excluded due to several reasons: on the one hand thermal properties have been determined by different approaches (indirect as well as measurements), one the other hand permafrost has been present for at least some ten thousand years. The warmer period during the Allerød (13.3–13.1 kyr BP), when the lake level was some 5 m higher than modern and flooded the coring site at that time (Schwamborn et al., 2008, 2012), was studied by different model runs and showed that there is no influence on the current temperature field anymore.

Therefore we conclude that past surface temperature changes are most like to be responsible for the temperature variation with depth. As a result we propose a possible large amplitude of the Little Ice Age (LIA) of 3.5 K lower temperature during the 1500–1900 period GST than today's mean GST. A subsequent still cool period until 1950 of 2.5 K lower than today is able to approximately explain the observed temperature profile. Though data are sparse in this area of Siberia, there are some other indications for low LIA temperatures. Mann et al. (2009) includes some tree ring density reconstructions from Northern Siberia, which indicate temperature differences of more than −2.5 K with respect to the modern. In addition, the recently published CRUTEM4 the 10-yr averaged land surface temperature anomalies (Jones et al., 2012), now including many more sites from Siberia, show a strong warming of more than 1 K since 1970 in this area.

To obtain a overview on the uncertainties of prediction, we performed a Monte Carlo (MC) experiment. The setup was as following: as in the simulation presented above, the last glaciation cycle was parametrised as simple as possible, in this case a boxcar function. As the time of the postglacial warming is rather well constrained, we choose to vary only three parameters, the preglacial average temperature (PAT), the average glacial temperature (GAT) and the timing of the glacial initiation (TGI). Concerning the PAT it is well known, that due to the strong attenuation of temperature perturbations with time, only the temperature changes of the last glacial cycle play a significant role. Older variations may safely be approximated by an appropriate average temperature (see, e.g. Majorowicz et al., 2008). For the purposes followed here, even the variations during the glacial are accommodated easily this way. Though nearer to the present, even the steepness of the temperature rise during the glacial-interglacial transition plays a detectable but minor role. In particular, Rath et al. (2012) have shown that for very shallow boreholes as the one considered here, the joint effect of the glacial-interglacial complex is indistinguishable from an additional linear trend, or, more physically, to an additional heat flow density. Thus, we think this simple parametrisation as reasonable.

We assumed independent normal distributions for all three parameters, implying that they are characterized by their means $\hat{\mu}_i$ and standard deviations $\hat{\sigma}_i$. The values assumed are given in Table 6, while the generated distributions can be found in Fig. 9. The results are shown in Fig. 10. From these results we conclude that the uncertainties assumed for the more ancient GSTH produce a considerable spread in temperatures already in the first few hundreds of metres. This spread carries over to the depths of the lower limit of permafrost, which can be found in Fig. 11. Unfortunately the existing geophysical surveys do not extend beyond the lake area and its immediate surroundings, so that recent undisturbed permafrost extent could not be observed. However, the values in Fig. 11 largely agree with the values found in the literature for this area (Yershov, 1998).

6 Conclusions and outlook

Our results of 2-D numerical simulations of the temperature field in El'gygytgyn Crater indicate the permafrost depth and the talik dimensions around and below the lake basin, as well as the influence of past temperature changes. The temperature model suggests a permafrost depth surrounding the lake of 330–360 m. This result depends on the assumption of an ancient transient signal present in the temperature distribution that evolved from low temperatures during the last glacial maximum. MC simulations permitted a crude characterization of the uncertainties in permafrost depth. More recent signals in the temperature distribution presumably originate from the Little Ice Age and the recent global warming. In particular regarding the LIA, our comparison between data and modelling suggests a significant and persistent cooling during that time period. A possible bias by fluid flow can probably be excluded, because the regime below the active zone remained frozen at least for the last 10 kyr. The talik below the lake basin is pervasive and follows a normal temperature gradient of 3 °C per 100 m starting at 5.5 °C in the uppermost lake sediment layers.

Future studies are necessary to improve the interpretation of the very shallow temperature field. In particular, these will include additional forward modelling in order to improve our conceptual model, and assess the sensitivities of our results with respect to subsurface heterogeneity or possibly subsurface flow. Using more sophisticated inverse techniques will not only enable us to obtain a better characterization of the past surface temperature changes, but also to characterize the uncertainties involved. The annual variation visible in the high quality temperature monitoring data of the top 20 m was not investigated in this study. However, these observations could be used to retrieve valuable constraints for the very shallow subsurface properties.

Acknowledgements. Funding for this research was provided by the International Continental Scientific Drilling Program (ICDP), the US National Science Foundation (NSF), the German Federal Ministry of Education and Research (BMBF), the Alfred Wegener Institute (AWI), and GeoForschungsZentrum Potsdam (GFZ), the Russian Academy of Sciences Far East Branch (RAS FEB), the Russian Foundation for Basic Research (RFBR), and the Austrian Federal Ministry of Science and Research (BMWF). The down hole logging was performed by the ICDP Operational Support Group (OSG), while LacCore at the University of Minnesota, handled core curation. We appreciate the help of the El'gygytgyn Science Party at various stages, and in particular the efforts of Grigoriy Fedorov and Lutz Schirrmeister. We are also indebted to Lothar Ahrensmeier who performed the laboratory measurements, for which we also got valuable advice from Hossein Honarmand (TeKa Berlin). Volker Rath was funded by the Spanish Government by its Ramón y Cajal Program (Ministerio de Ciencia y Educación), project CCG10-UCM/ESP-5070 (Comunidad de Madrid/UCM), and project CGL2011-29672-C02-01 (Ministerio de Economía y Competitividad).

References

Asikainen, C., Francus, P., and Brigham-Grette, J.: Sedimentology, clay mineralogy and grain-size as indicators of 65 ka of climate change from El'gygytgyn Crater Lake, Northeastern Siberia, J. Paleolimnol., 37, 105–122, doi:10.1007/s10933-006-9026-5, 2007. 2614

Beck, A. E.: Methods for determining thermal conductivity and thermal diffusivity, in: Handbook of Terrestrial Heat-flow Density Determination, edited by: Hänel, R., Rybach, L., and Stegena, L., Kluwer, Dordrecht, 1988. 2614

Beck, A. E., Shen, P. Y., Beltrami, H., Mareschal, J.-C., Šafanda, J., Sebagenzi, M. N., Vasseur, G., and Wang, K.: A comparison of five different analyses in the interpretation of five borehole temperature data sets, Palaeogeogr. Palaeoclim., 98, 101–112, 1992. 2610

Beltrami, H. and Mareschal, J.-C.: Recent warming in Eastern Canada inferred from geothermal measurements, Geophys. Res. Lett., 18, 605–608, 1991. 2610

Demezhko, D. Y., Ryvkin, D. G., Outkin, V. I., Duchkov, A. D., and Balobaev, V. T.: Spatial distribution of Pleistocene/Holocene warming amplitudes in Northern Eurasia inferred from geothermal data, Clim. Past, 3, 559–568, doi:10.5194/cp-3-559-2007, 2007. 2610

Erbas, K.: Eine universelle Methode zur Bestimmung der Wärmeleitfähigkeit aus Aufheizkurven konstant geheizter Zylinderquellen, Dissertation, Technische Universität Berlin, Berlin, 2001. 2612

Fukusako, S.: Thermophysical properties of ice, snow, and sea ice, Int. J. Thermophys., 11, 353–372, 1990. 2614

Galushkin, Y.: Numerical simulation of permafrost evolution as a part of sedimentary basin modeling: permafrost in the Pliocene – Holocene climate history of the Urengoy field in the West Siberian basin, Can. J. Earth Sci., 34, 935–948, 1997. 2609

Ge, S., McKenzie, J., Voss, C., and Wu, Q.: Exchange of groundwater and surface-water mediated by permafrost response to seasonal and long term air temperature variation, Geophys. Res. Lett., 38, L14402, doi:10.1029/2011GL047911, 2011. 2615

Gebhardt, C., Niessen, F., and Kopsch, C.: Central ring structure identified in one of the world's best-preserved impact craters, Geology, 34, 145–148, doi:10.1130/G22278.1, 2006. 2614

Gebhardt, C., Wennrich, V., Kueck, J., Niessen, F., Melles, M., and the El'gygytgyn Scientific Party: Physical properties, downhole logging and seismic data from deep drilling in Lake El'gygytgyn, Chukotka, NE Siberia – initial results, in: Geophysical Research Abstracts, EGU General Assembly 2010, Vol. 12, EGU2010-12579, 2010. 2614

González-Rouco, J. F., Beltrami, H., Zorita, E., and Stevens, M. B.: Borehole climatology: a discussion based on contributions from climate modeling, Clim. Past, 5, 97–127, doi:10.5194/cp-5-97-2009, 2009. 2610

Goutorbe, B., Poort, J., Lucazeau, F., and Raillard, S.: Global heat flow trends resolved from multiple geological and geophysical proxies, Geophys. J. Int., 187, 1405–1419, doi:10.1111/j.1365-246X.2011.05228.x, 2011. 2616

Hartmann, A., Pechnig, R., and Clauser, C.: Petrophysical analysis of regional-scale thermal properties for improved simulations of geothermal installations and basin-scale heat and fluid flow, Int. J. Earth Sci., 97, 421–433, doi:10.1007/s00531-007-0283-y, 2008. 2613

Holmén, J., Benabderrahmane, H., Buoro, A., and Brulhet, J.: Modelling of permafrost freezing and melting and the impact of a climatic cycle on groundwater flow at the Meuse/Haute-Marne site, Phys. Chem. Earth, 36, 1531–1538, doi:10.1016/j.pce.2011.10.021, 2011. 2609

Jones, P. D., Lister, D. H., Osborn, T. J., Harpham, C., Salmon, M., and Morice, C. P.: Hemispheric and large-scale land-surface air temperature variations: an extensive revision and an update to 2010, J. Geophys. Res., 117, D05127, doi:10.1029/2011JD017139, 2012. 2619

Juschus, O., Pavlov, M., Schwamborn, G., Preusser, F., Fedorov, G., and Melles, M.: Late quaternary lake-level changes of Lake El'gygytgyn, NE Siberia, Quaternary Res., 76, 441–451, doi:10.1016/j.yqres.2011.06.010, 2011. 2615

Kukkonen, I. T.: Vertical variation of apparent and palaeoclimatically corrected heat flow densities in the Central Baltic Shield, J. Geodyn., 8, 33–53, 1987. 2615

Lemke, P., Ren, J., Alley, R., Allison, I., Carrasco, J., Flato, G., Fujii, Y., Kaser, G., Mote, P., Thomas, R., and Zhang, T.: Observations: changes in snow, ice and frozen ground, in: Climate Change 2007: The Physical Science Basis, edited by: Solomon, S., Qin, D., Manning, M., Chen, Z., Marquis, M., Averyt, K., Tignor, M., and Miller, H., Cambridge University Press, Cambridge, UK and New York, NY, USA, 2007. 2609

Ling, F. and Zhang, J.: A numerical model for surface energy balance and thermal regime of the active layer and permafrost containing unfrozen water, Cold Reg. Sci. Technol., 38, 1–15, doi:10.1016/S0165-232X(03)00057-0, 2004. 2614

Lunardini, V. J.: Freezing of soil with an unfrozen water content and variable thermal properties, Tech. Rep. 88-2, US Army Cold Regions Research and Engineerimg Laboratory (CRREL), 1988. 2614

Majorowicz, J., Šafanda, J. S., and Torun-1 Working Group: Heat flow variation with depth in Poland: evidencefrom equilibrium temperature logs in 2.9-km-deep well Torun-1, Int. J. Earth Sci., 97, 307–315, doi:10.1007/s00531-007-0210-2, 2008. 2619

Mann, M. E., Zhang, Z., Rutherford, S., Bradley, R. S., Hughes, M. K., Shindell, D., Ammann, C., Faluvegi, G., and Ni, F.: Global signatures and dynamical origins of the Little Ice Age and Medieval climate anomaly, Science, 326, 1256–1230, doi:10.1126/science.1177303, 2009. 2619

Mayr, S. I., Wittmann, A., Burkhardt, H., Popov, Y., Romushkevich, R., Bayuk, I., Heidinger, P., and Wilhelm, H.: Integrated interpretation of physical properties of rocks of the borehole Yaxcopoil-1 (Chicxulub impact structure), J. Geophys. Res., 113, B07201, doi:10.1029/2007JB005420, 2008. 2614

Melles, M.: Sedimentological bulk parameters from core profile Lz1024 in lake El'gygytgyn, Siberia, doi:10.1594/PANGAEA.510816, 2006. 2614

Melles, M., Brigham-Grette, J., Minyuk, P., Koeberl, C., Andreev, A., Cook, T., Fedorov, G., Gebhardt, C., Haltia-Hovi, E., Kukkonen, M., Nowaczyk, N., Schwamborn, G., Wennrich, V., and Party, E. S.: The Lake Elgygytgyn scientific drilling project conquering Arctic challenges in continental drilling, Sci. Drill., 11, 29–40, 2011. 2635

Melles, M., Brigham-Grette, J., Minyuk, P. S., Nowaczyk, N. R., Wennrich, V., DeConto, R. M., Anderson, P. M., Andreev, A. A., Coletti, A., Cook, T. L., Haltia-Hovi, E., Kukkonen, M., Lozhkin, A. V., Rosén, P., Tarasov, P., Vogel, H., and Wagner, B.: 2.8 MillionYears of Arctic climate change from Lake El'gygytgyn, NE Russia, Science, doi:10.1126/science.1222135, in press, 2012. 2609

Miller, G., Brigham-Grette, J., Anderson, L., Bauch, D., Douglas, M., Edwards, M., Elias, S., Finney, B., Funder, S., Herbert, T., Hinzman, L., Kaufman, D., MacDonald, G., Robock, A., Serreze, M., Smol, J., Spielhagen, R., Wolfe, A., and Wolff, E.: Past climate variability and change in the Arctic and at high latitudes, a report by the US Climate Change Program and Subcommittee on Global Change, chap. Temperature and Precipitation History of the Arctic, Research, US Geological Survey, Reston, 2009. 2609

Miller, G., Brigham-Grette, J., Alley, R., Anderson, L., Bauch, H., Douglas, M., Edwards, M., Elias, S., Finney, B., Fitzpatrick, J., Funder, S., Herbert, T., Hinzman, L., Kaufman, D., MacDonald, G., Polyak, L., Robock, A., Serreze, M., Smol, J., Spielhagen, R., White, J., Wolfe, A., and Wolff, E.: Temperature and precipitation history of the Arctic, Quaternary Sci. Rev., 29, 1679–1715, doi:10.1016/j.quascirev.2010.03.001, 2010a. 2610, 2618

Miller, G. H., Alley, R. B., Brigham-Grette, J., Fitzpatrick, J. J., Polyak, L., Serreze, M. C., and White, J. W.: Arctic amplification: can the past constrain the future?, Quaternary Sci. Rev., 29, 1779–790, doi:10.1016/j.quascirev.2010.02.008, 2010b. 2609, 2610

Mottaghy, D. and Rath, V.: Latent heat effects in subsurface heat transport modeling and their impact on paleotemperature reconstructions, Geophys. J. Int., 164, 236–245, doi:10.1111/j.1365-246X.2005.02843.x, 2006. 2609, 2611, 2614

Nolan, M.: Analysis of local AWS and NCEP/NCAR reanalysis data at Lake El'gygtytgyn, and its implications for maintaining multi-year lake-ice covers, Clim. Past Discuss., 8, 1443–1483, doi:10.5194/cpd-8-1443-2012, 2012. 2615

Nolan, M. and Brigham-Grette, J.: Basic hydrology, limnology, and meteorology of modern Lake El'gygytgyn, Siberia, J. Paleolimnol., 37, 17–35, doi:10.1007/s10933-006-9020-y, 2007. 2615

Osterkamp, T. E. and Gosink, J. P.: Variations in permafrost thickness in response to changes in paleoclimate, J. Geophys. Res., 96, 4423–4434, 1991. 2609

Pollack, H. N., Hurter, S. J., and Johnson, J. R.: Heat flow from the Earth's interior: analysis of the global data set, Rev. Geophys., 31, 267–280, doi:10.1029/93RG01249, 1993. 2616

Popov, Y. A., Pribnow, D. F. C., Sass, J. H., Williams, C. F., and Burkhardt, H.: Characterization of rock thermal conductivity by high-resolution optical scanning, Geothermics, 28, 253–276, 1999. 2613

Popov, Y. A., Tertychnyi, V., Romushkevich, R., Korobkov, D., and Pohl, J.: Interrelations between thermal conductivity and other physical properties of rocks: experimental data, Pure Appl. Geophys., 160, 1137–1161, 2003. 2614

Putkonen, J.: Determination of frozen soil thermal properties by heated needle probe, Permafrost Periglac., 14, 343–347, doi:10.1002/ppp.465, 2003. 2612

Rath, V. and Mottaghy, D.: Smooth inversion for ground surface temperature histories: estimating the optimum regularization parameter by generalized cross-validation, Geophys. J. Int., 171, 1440–1448, doi:10.1111/j.1365-246X.2007.03587.x, 2007. 2610, 2611

Rath, V., Wolf, A., and Bücker, M.: Joint three-dimensional inversion of coupled groundwater flow and heat transfer based on automatic differentiation: sensitivity calculation, verification, and synthetic examples, Geophys. J. Int., 167, 453–466, doi:10.1111/j.1365-246X.2006.03074.x, 2006. 2613

Rath, V., González Rouco, J. F., and Goosse, H.: Impact of postglacial warming on borehole reconstructions of last millennium temperatures, Clim. Past, 8, 1059–1066, doi:10.5194/cp-8-1059-2012, 2012. 2610, 2620

Saito, K., Kimoto, M., Zhang, J., Takata, K., and Emori, S.: Evaluating a high-resolution climate model: simulated hydrothermal regimes in frozen ground regions and their change under the global warming scenario, J. Geophys. Res.-Earth, 112, F02S11, doi:10.1029/2006JF000577, 2007. 2609

Schwamborn, G., Fedorov, G., Schirrmeister, L., Meyer, H., and Hubberten, H.-W.: Periglacial sediment variations controlled by late quaternary climate and lake level change at Elgygytgyn Crater, Arctic Siberia, Boreas, 37, 55–65, 2008. 2619

Schwamborn, G., Fedorov, G., Ostanin, N., Schirrmeister, L., Andreev, A., and the El'gygytgyn Scientific Party: Alluvial fan dynamics in the El'gygytgyn Crater: implications for the 3.6 Ma old sediment archive, Clim. Past Discuss., 8, 2187–2222, doi:10.5194/cpd-8-2187-2012, 2012. 2612, 2619

Serreze, M. C. and Barry, R. G.: Processes and impacts of Arctic amplification: a research synthesis, Global Planet. Change, 77, 85–96, doi:10.1016/j.gloplacha.2011.03.004, 2011. 2609

Serreze, M., Barrett, A., Slater, A., Steele, M., Zhang, J., and Trenberth, K.: The large-scale energy budget of the Arctic, J. Geophys. Res., 112, D11122, doi:10.1029/2006JD008230, 2007. 2609

Shen, P. Y. and Beck, A. E.: Least squares inversion of borehole temperature measurements in functional space, J. Geophys. Res., 96, 19965–19979, 1991. 2610

Smerdon, J. E., Pollack, H. N., Cermak, V., Enz, J. W., Kresl, M., Šafanda, J., and Wehmiller, J. F.: Air-ground temperature coupling and subsurface propagation of annual temperature signals, J. Geophys. Res., 109, D21107, doi:10.1029/2004JD005056 , 2004. 2615

Smerdon, J. E., Pollack, H. N., Cermak, V., Enz, J. W., Kresl, M., Šafanda, J., and Wehmiller, J. F.: Daily, seasonal and annual relationships between air and subsurface temperatures, J. Geophys. Res., 111, D07101, doi:10.1029/2004JD005578, 2006. 2615

Stieglitz, M. and Smerdon, J.: Characterizing land-atmosphere coupling and the implications for subsurface thermodynamics, J. Climate, 20, 21–37, doi:10.1175/JCLI3982.1, 2007. 2615

Vincent, W. F. and Laybourn-Parry, J. (Eds.): Polar Lakes and Rivers: Limnology of Arctic and Antarctic Aquatic Ecosystems, Oxford University Press, Oxford, UK, 2008. 2615

Yershov, E. D.: General Geocryology, Cambridge University Press, Cambridge, UK, 1998. 2616, 2620

CPD
8, 2607–2644, 2012

Table 1. Summary of the different measured thermal conductivity values λ ($\mathrm{W\,m^{-1}\,K^{-1}}$) of the sample No. 28(2) from the permafrost borehole 5011-3. ϕ is porosity, which can be estimated from the ratio of volume and mass of the sample (ϕ_a), or from thermal conductivity (ϕ_b). Based on these, the corresponding matrix thermal conductivities $\lambda_m^{a,b}$ can be determined. FSLS: full space line source, HSLS: half space line source.

State	$\lambda_{\mathrm{total}}^{\mathrm{FSLS}}$	λ_m^a	λ_m^b	$\lambda_{\mathrm{total}}^{\mathrm{HSLS}}$	ϕ^a (–)	ϕ^b (–)
–					0.29	0.27
Unfrozen	1.5 ± 0.3	2.15	2.23	1.25 ± 0.02		
Frozen	2.25 ± 0.01	2.23	2.23	n/a		

CPD
8, 2607–2644, 2012

CPD
8, 2607–2644, 2012

Lake El'gygytgyn site: thermal modelling

D. Mottaghy et al.

Table 2. Summary of the different measured thermal conductivity values λ ($\mathrm{W\,m^{-1}\,K^{-1}}$) for the two samples from unit 3 and 4, respectively. Porosity ϕ is determined from saturated and dry thermal conductivity measurements.

	λ_{dry}	$\lambda_{min-max,dry}$	λ_{sat}	$\lambda_{min-max,sat}$	ϕ from λ (–)	λ_{matrix}
Sample 1, C104Q	1.69	1.62–1.82	2.20	2.01–2.59	0.08	2.48
Sample 2, C170Q	1.84	1.65–2.13	2.18	1.94–2.42	0.06	2.35

Table 3. Properties of the 2-D model. In case of the transient modelling, the temperature at the upper boundary is time dependent as shown in Fig. 7.

Parameter	Value
Mesh Size	465 × 174
Model Size	16368 m × 835 m
Resolution	35.2 m × 4.8 m
Geological Units	5
Thermal conductivity	$f(T)$ Thermal boundary condition Top: $T(t)$, bottom: constant q
Basal heat flow q	70 mW m^{-2}
Surface temperature	−6.7 °C
Lake bottom temperature	5.5 °C

CPD
8, 2607–2644, 2012

Table 4. The five lithological units and their thermal parameters. Thermal conductivity λ is varied within the given ranges which is ±20 % of the mean value. ϕ is porosity, λ_{bulk} denotes the total (bulk) thermal conductivity for the unfrozen material, and $\rho\ c_p$ is volumetric heat capacity. The values in bold correspond to the measured properties of the sample from unit 1, 3, and 4.

Unit	ϕ (–)	λ_m ($W\,m^{-1}\,K^{-1}$)	λ_{bulk} ($W\,m^{-1}\,K^{-1}$)	$\rho\ c_p$ ($MJ\,m^{-3}\,K^{-1}$)
Unit 1 (Quarternary)	0.40	1.8–**2.2**–2.6	1.1–1.3–1.5	2.3
Unit 2 (Pliocene)	0.30	1.6–2.0–2.4	1.2–1.4–1.6	2.3
Unit 3 (Impact rocks)	0.10	2.0–**2.5**–3.0	1.8–2.2–2.6	2.3
Unit 4 (Impact rocks)	0.06	1.9–**2.4**–2.9	1.8–2.2–2.6	2.3
Unit 5 (Volcanic bedrock)	0.05	1.8–2.3–2.8	1.7–2.2–2.6	2.3

CPD
8, 2607–2644, 2012

Table 5. Depth of permafrost base for the different simulations at borehole 5011-3. S-S: steady-state.

Simulation type	S-S mean TC	S-S lower TC	S-S higher TC	Transient today	Transient 7 kyr BP	Transient 20 kyr BP
Base of permafrost	180 m	155 m	195 m	335 m	415 m	475 m

CPD
8, 2607–2644, 2012
Lake El'gygytgyn site: thermal modelling
D. Mottaghy et al.

Table 6. Parameters used for the Monte-Carlo simulations in this study. PAT is the long term average pre-glacial ground surface temperature, while GAT denotes the minimum temperature of the simplified glacial GSTH. This boxcar-like period of low temperatures begins at TGI. All parameters were assumed to be independently and normally distributed.

	PAT °C	GAT °C	TGI kyr
$\hat{\mu}$	−12	−24	80
$\hat{\sigma}$	4	5	20

CPD
8, 2607–2644, 2012

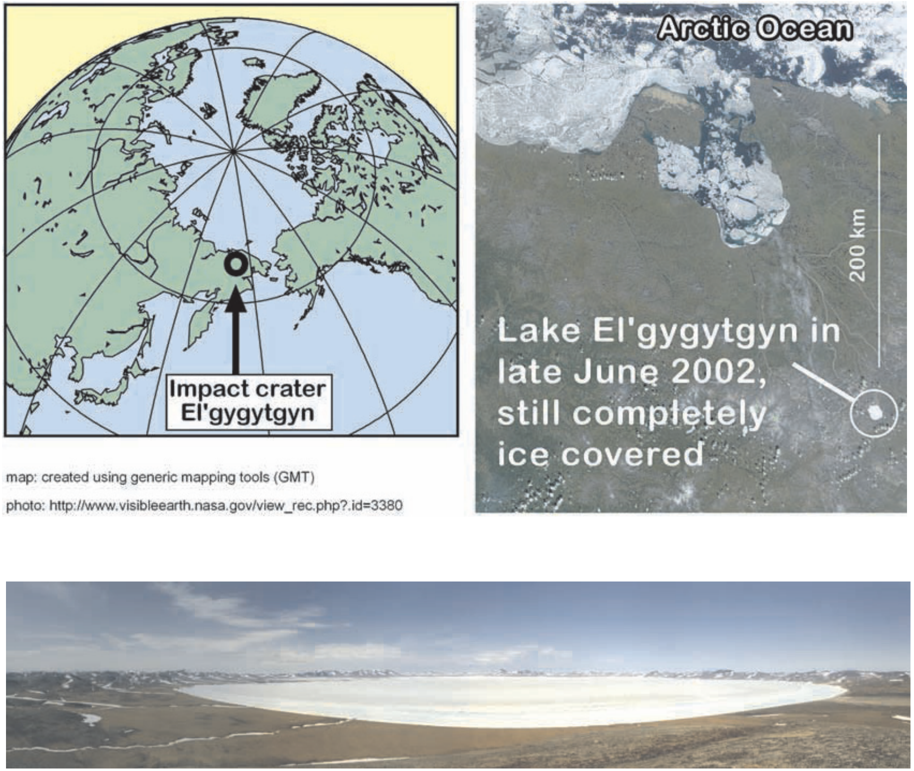

Fig. 1. Location and panorama view of the Lake El'gygytgyn (photo by S. Quart, 2003).

CPD
8, 2607–2644, 2012
Lake El'gygytgyn site: thermal modelling
D. Mottaghy et al.

Title Page
Abstract | Introduction
Conclusions | References
Tables | Figures
◀| |▶
◀ ▶
Back | Close
Full Screen / Esc
Printer-friendly Version
Interactive Discussion

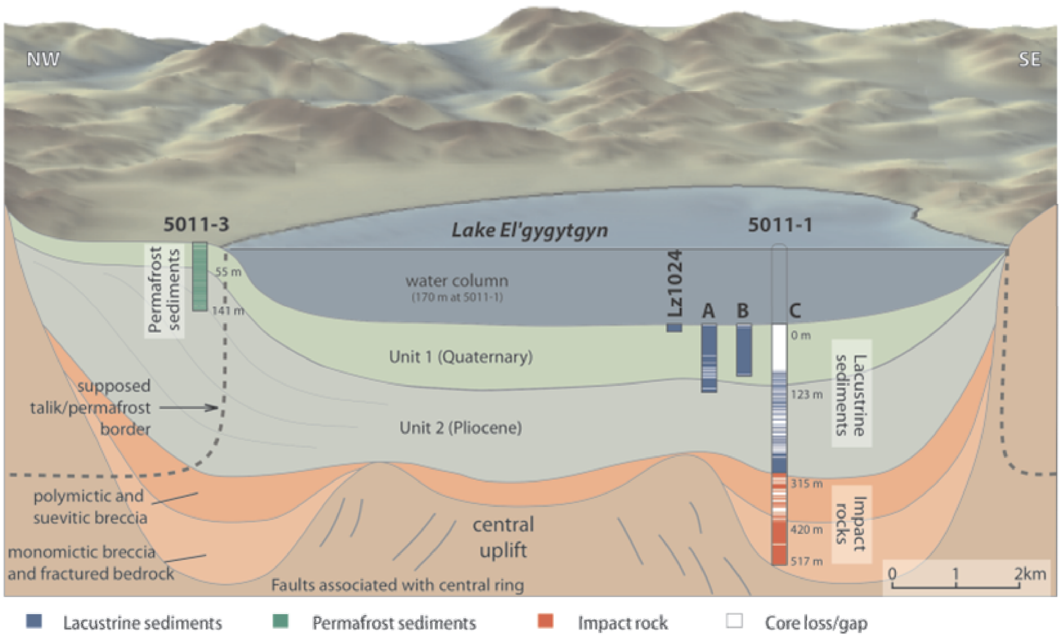

Fig. 2. Basin scheme of the Lake El'gygytgyn site with the digital elevation model in the background. The numerical model is based on this conceptual model (Melles et al., 2011).

CPD
8, 2607–2644, 2012

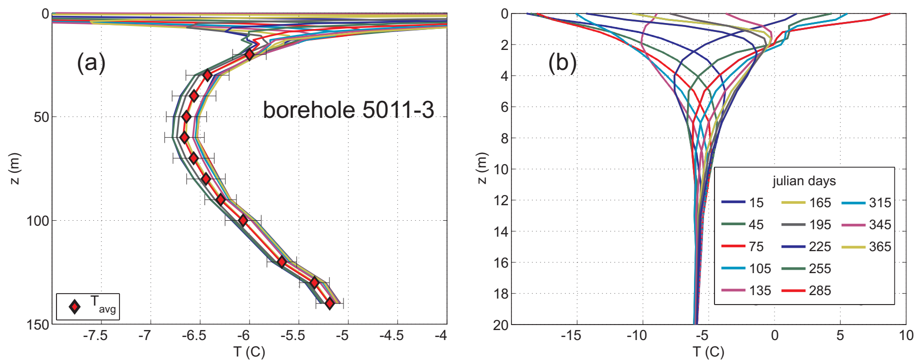

Fig. 3. Selection of the temperatures logs in the permafrost borehole 5011-3 during the year 2010.

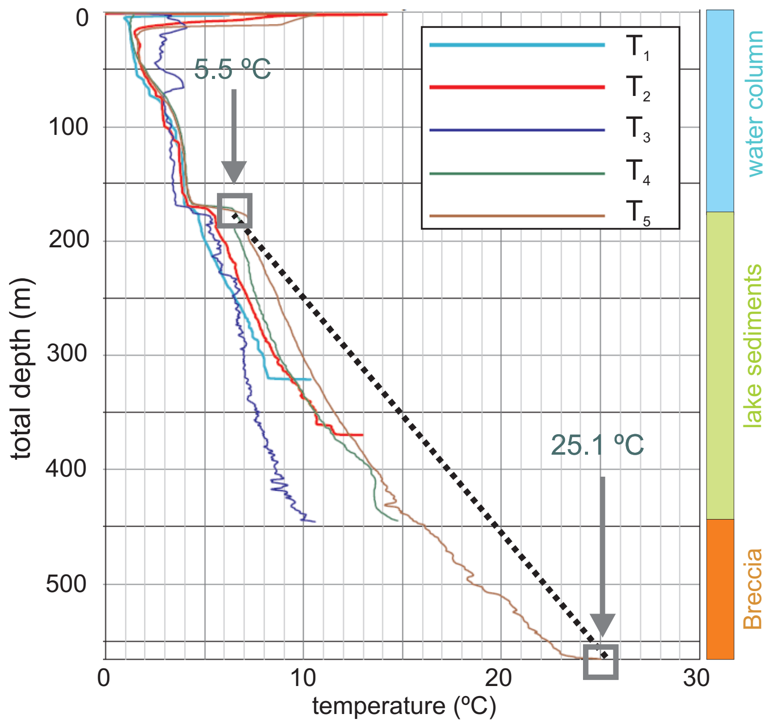

Fig. 4. Temperature logs in borehole ICDP site 5011-1. Temp_5 is the most reliable, and thus is used for estimating the temperature gradient (data by ICDPOSG, 2009).

CPD
8, 2607–2644, 2012

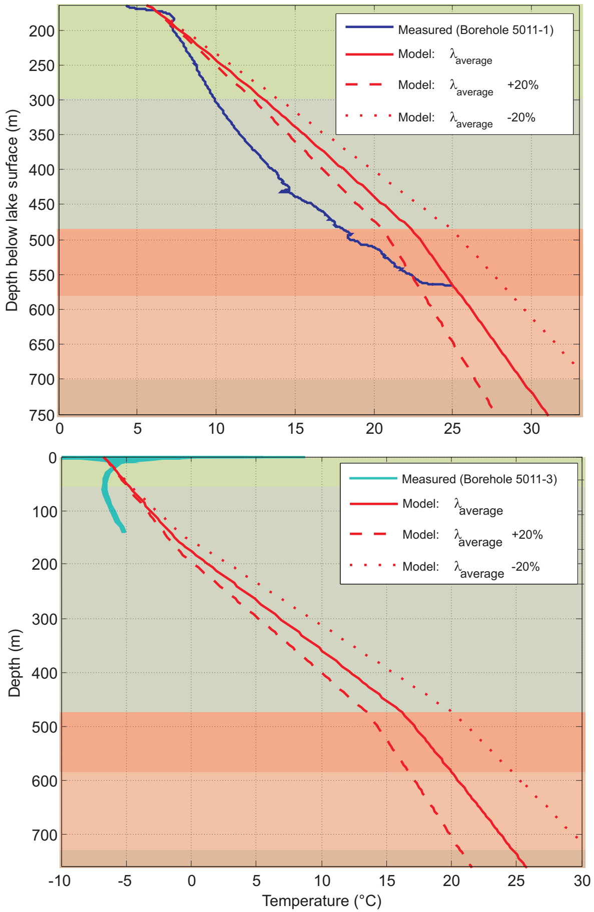

Fig. 5. Modelled temperatures at borehole locations 5011-1 and 5011-3. The dashed lines show the sensitivity to thermal conductivity variations. The colours indicate the units as in Fig. 2.

CPD
8, 2607–2644, 2012

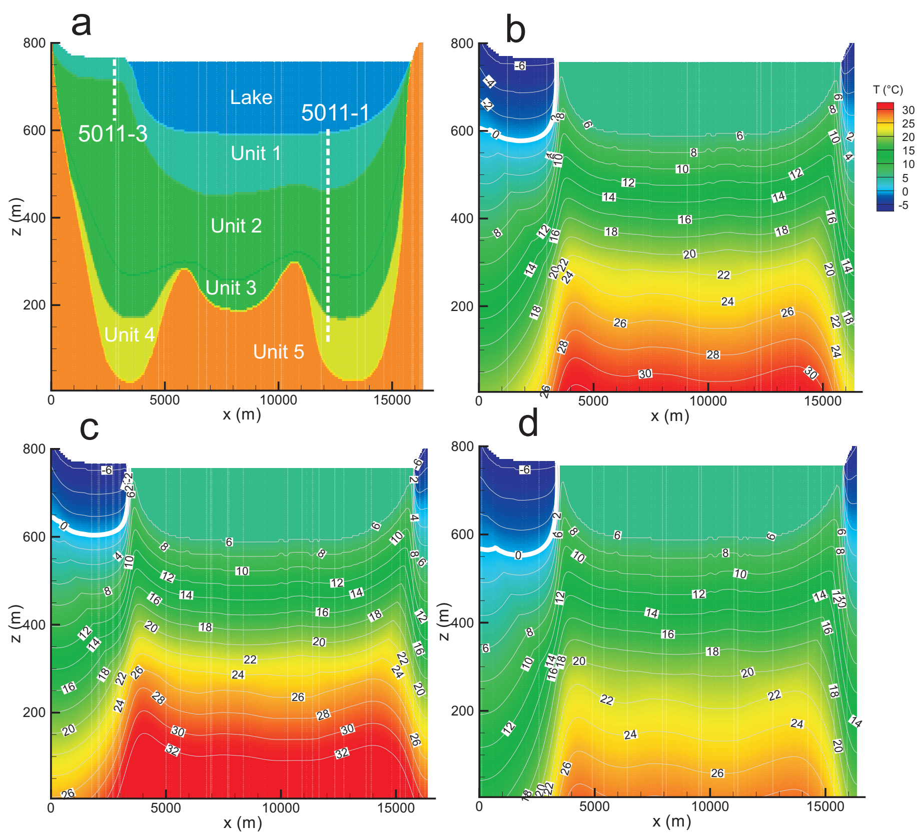

Fig. 6. (a) The model and its units. The temperature field using **(b)** the mean value, **(c)** lower thermal conductivity, and **(d)** higher thermal conductivity.

CPD
8, 2607–2644, 2012

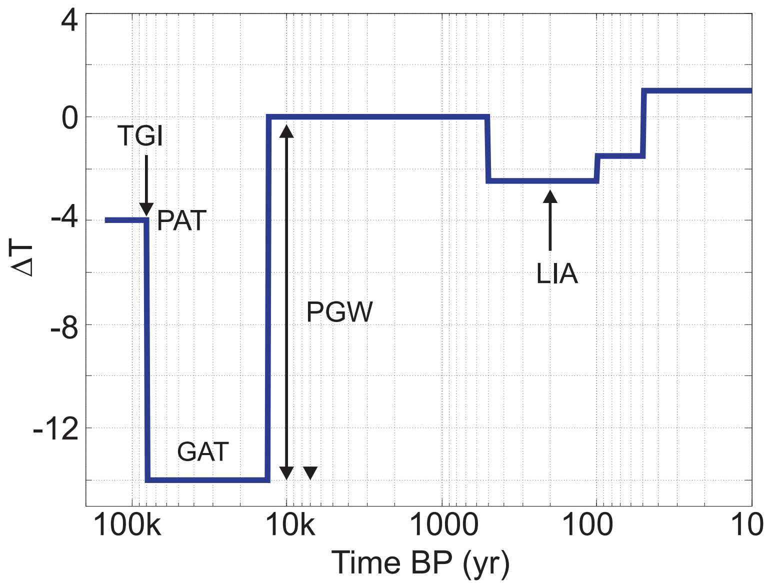

Fig. 7. The simplified boxcar model used in the transient simulations. The magnitude of the post-glacial (PGW) warming is influencing the gradient of the deeper part of the temperature profile in Fig. 3, whereas the magnitude of the LIA and the recent temperature changes are responsible for the curvature in the shallow domain. The mean GST before the LIA is taken as a reference. PAT is the preglacial average temperature, TGI is the time of glacial inception, and GAT the average glacial temperature.

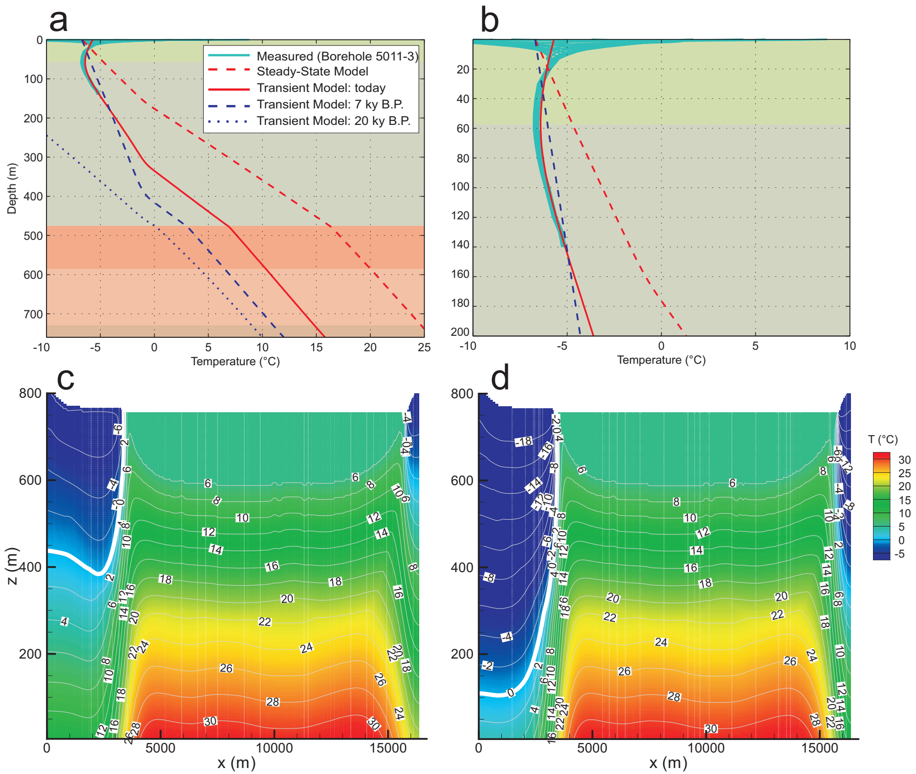

Fig. 8. Results from the transient simulations. Temperature profiles at borehole 5011-3 showing **(a)** the whole model depth, and **(b)** only the upper part. The temperature field of the model **(c)** today, and 20 kyr BP **(d)**.

CPD
8, 2607–2644, 2012

Lake El'gygytgyn site: thermal modelling

D. Mottaghy et al.

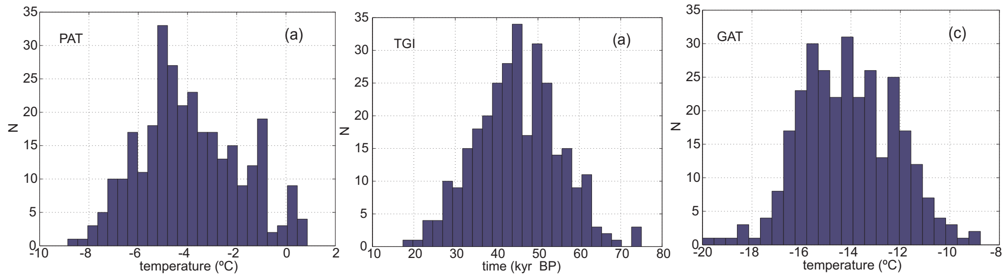

Fig. 9. Histograms of the parameter values for the MC simulations in Fig. 10.

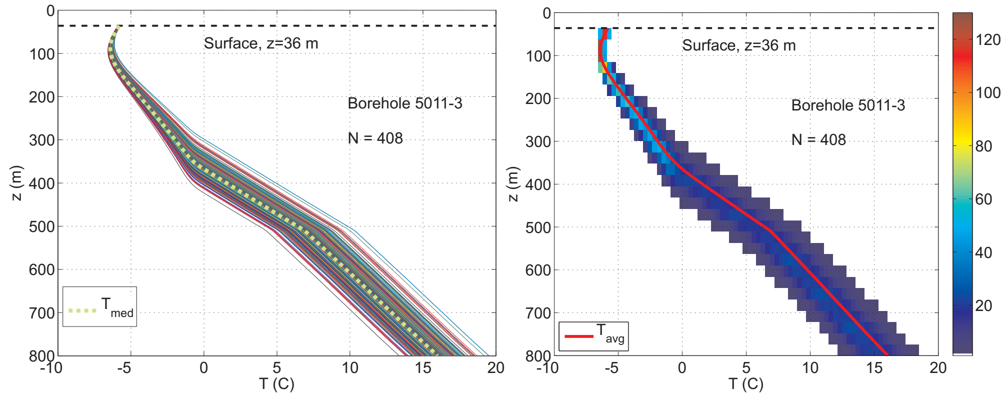

Fig. 10. Results from the MC simulations for the 5011-3 borehole. The parameter values assumed are given in Table 6.

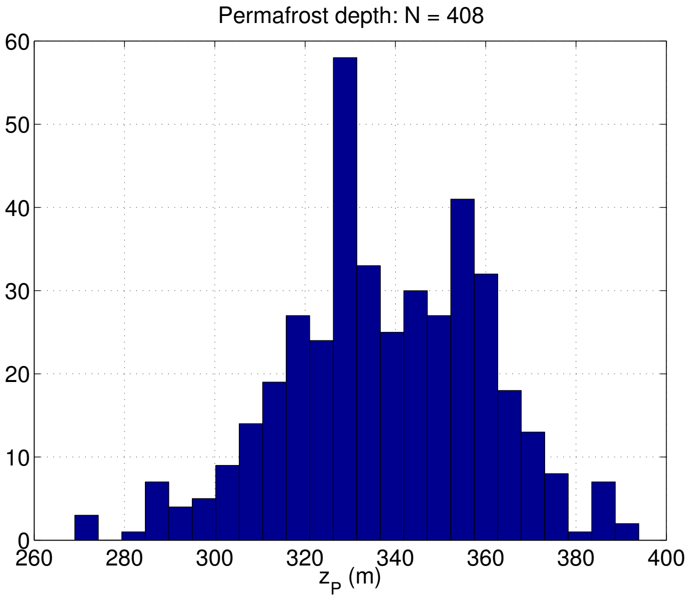

Fig. 11. Histograms of the depth to the lower boundary of permafrost for the MC simulations in Fig. 10.

CPD
8, 2607–2644, 2012